

Nanocatalytic Efficacy of Silver Nanoparticles Fabricated using *Chaetomorpha antennina* Algal Extract, Their Characterization, and Its Applications

A. Kingslin¹, K. Kalimuthu^{2*}, P. Viswanathan²

¹St Mary Goretty Higher Sec. School, Manalikai, Kanyakumari, Tamil Nadu, India

²Plant tissue culture Division, PG and Research Department of Botany, Government Arts College (Autonomous), Coimbatore, Tamilnadu, India

Received 5 June 2021, accepted in final revised form 12 October 2021

Abstract

Silver nanoparticles (SNPs) were synthesized by using an aqueous extract of the green seaweed *Chaetomorpha antennina*. Synthesized SNPs were characterized by UV-Visible spectroscopy, FTIR, XRD, FESEM, EDAX, and DLS with Zeta potential techniques. The formation of SNPs is confirmed by the appearance signatory brown color of the solution and a characteristic peak at 452 nm in the UV-Vis spectrum. FTIR spectrum indicated 11 intense peaks with different functional groups in capping the nanoparticles. The SNP lattice is unaffected by other molecules in the algal extract, as revealed in the XRD pattern, and the average size was 21 nm according to the full width at half minimum. FESEM images revealed that the synthesized SNPs are spherical in morphology, with sizes ranging from 69.99 to 99.19 nm. The EDX result indicates that Ag-NPs display an absorption peak at 3 keV shows the presence of the silver element. The obtained zeta potential value of SNPs through the DLS method was -27.4 mV. The seedling growth was positively affected by a specific concentration of SNPs. In the antioxidant activity, the IC₅₀ value was 384.13 µg/mL. The SNPs react with earthworm *Lampito mauritii* in the mortality rate of 25 % and 100 % for 3 min.

Keywords: Green synthesis; Silver nanoparticles; *Chaetomorpha antennina*; Characterization; Antioxidant activity.

© 2022 JSR Publications. ISSN: 2070-0237 (Print); 2070-0245 (Online). All rights reserved.
doi: <http://dx.doi.org/10.3329/jsr.v14i1.53782> J. Sci. Res. **14** (1), 343-362 (2022)

1. Introduction

Studying and utilizing extremely small things is the basis of nanotechnology and nanoscience, which can be applied to many other fields. The green synthesis of nanoparticles from plant sources might be one of these interventions [1]. Many nanotechnologies are used, ranging from traditional chemical applications to medical and environmental technologies [2]. AgNPs have contributed to a wide range of applications, including drug delivery [3], ointments, nanomedicine [4], agriculture, cosmetics [5], textiles [6], food industry, photocatalytic organic dye-degradation activity [7],

* Corresponding author: kalimuthu@icloud.com

antioxidants [8], and antimicrobial agents [9]. Further, the green synthesis of nanoparticles is also regarded as eco-friendly and cost-effective due to the small number of harmful chemicals released into the environment [10]. Plant-mediated synthesis of nanoparticles is a comparatively underexploited field and are recently receive ample attention compared to microorganism-assisted synthesis. By using various plant extracts, AgNPs have been well synthesized [11-15]. All these researches are confined to land plants, but only restricted reports are accessible to synthesize nanoparticles from marine plants [16-19]. Noteworthy secondary metabolites with therapeutic values are produced by marine macroalgae [20,21].

Seaweeds are large marine macroalgae that are multicellular and macroscopic. Marine algae are an immensely assorted diversified group of aquatic plants comprising a few thousand species. Seaweeds have bioactive principles with a tremendous health perspective. Several chemically novel compounds of marine origin with various bioactivities have been isolated, and many of them are under investigation and/or being developed as new pharmaceuticals [22-25]. Around 2400 marine natural bioactive compounds were distinguished as secondary metabolites isolated from seaweeds of subtropical and tropical populations with a broad range of biofunctional properties. As an effect of a growing call for biodiversity in the screening applications looking for healing drugs from herbal products, there is increasing attention in marine organisms, particularly marine algae. Screening of seaweeds for pharmaceutical activities and bioactive components is pretty imperative. Many drugs are synthesized from marine seaweeds beneficially by pharmaceutical industries. There is an ever-increasing demand and need for new bioactive drugs to control many malignant tumors.

Chaetomorpha antennina is a green alga coming under the family Cladophoraceae. This species in the genus is made up of macroscopic filaments of cylindrical cells. The genus is characterized by its unbranched filaments, making it distinctive. The biological activities of *C. antennina* are antibacterial [26], antiplasmodial [27], and antioxidant activity [28] etc. This species is rich in phytoconstituents like alkaloids, steroids, cardiac glycosides, and saponins [29]. *Chaetomorpha*, also known as Spaghetti algae or green hair algae, is a macroalga for a refugium. *Chaetomorpha* assimilates nitrate and phosphate from refugium and grows fastly. It also chelates heavy metals like copper and zinc in a water-based solution. It contains a heparin-like polysaccharide. *Chaetomorpha* has the potential to be used as an antibacterial agent [30]. Based on our literature search, there has been no evidence of silver nanoparticles studies in *C. antennina*. The present research work relied on the collection, identification, green synthesis, and Characterization of silver nanoparticles and their seed germination activities, earthworm toxicology, and antioxidant activity of green algae *Chaetomorpha antennina* (Bory de Saint-Vincent) Kutz.

2. Materials and Methods

2.1. Collection and identification

The fresh seaweed *Chaetomorpha antennina* (Bory de Saint-Vincent) Kutz. was collected from the Kanyakumari coast, Tamil Nadu, South India. The samples were brought to the laboratory in polythene bags and cleaned thoroughly with fresh water to remove adhering debris and associated biota. The algae were identified and authenticated by Botanical Survey of India, Southern region, Coimbatore 641013 with the letter-number S1/SRC/5/23/2014-15/Tech/851 dated 22nd August 2014 was dried in the shade at room temperature for further use (Fig. 1).



Fig. 1. *Chaetomorpha antennina*- Habit.

2.2. Preparation of seaweed extract

The seaweed *C. antennina* was washed thoroughly with Milli Q water to remove extraneous materials, and the log of the washed seaweed was finely cut into small pieces and stirred with 100 mL. The sterile Milli Q water for 1min and kept in a water bath at 4 °C for 20 min. Finally, the extract was filtered with Whatman no. 1 filter paper. The filtrate is employed as a reducer and stabilizer.

2.3. Biosynthesis of silver nanoparticles (SNPs)

For the biosynthesis of SNPs, 50 mL aqueous seaweed extract *C. antennina* was mixed with 50 mL of 1 mM AgNO₃ solution stirred well for 1 min kept in a water bath at 60 °C for 1 h, and incubated in the dark at normal temperature. By observing the change in color of the solution, it can be determined that AgNO₃ was bioreduced into AgNPs.

2.4. Characterization techniques

2.4.1. UV- visible spectroscopy analysis

The reduction process for the formation of SNPs in solution was monitored on a Perkin-Elmer UV-VIS Spectrometer Lambda – 35 to know the kinetic behavior of the AgNPs. The reaction of the solution was analyzed at different reaction times in the wavelength ranges between 200 and 800 nm at a scan speed of 480 nm/min. The spectrophotometer was equipped with "UV Winlab" software to record and analyze data. Baseline correction of the spectrometer was carried out by using a blank reference. The UV-Vis absorption spectra of extract SNPs were recorded, along with the resulting data recorded in graphical format, headings were taken for all the concentrations mentioned. To study the effect of time duration on SNP formation, the reaction solution was incubated at specific time intervals of 0, 1, 6, 12, and 24 h for each of the concentrations.

2.4.2. Fourier transform infrared (FTIR) measurement

FTIR measurements were carried out to investigate and predict any physicochemical interactions between different components in a formulation in the dried biomass of the extract-treated with AgNO₃ to find out the compound responsible for the synthesis of SNPs. FTIR measurements were taken for the SNPs synthesized after 0, 6, 12, and 24 h of reaction. These measurements were carried using an FTIR PERKIN ELMER instrument with a wavelength range of 4000 to 400 nm where the samples were incorporated with KBr pellets to acquire the spectra. The obtained results were compared with shifts in functional peaks.

2.4.3. X-ray diffraction measurement (XRD)

The phase evolution of *C. antennina* SNPs was studied by X-ray diffraction techniques (Philips PAN Analytical, The Netherland) using Cu α radiation. The Ag samples were scanned in the 2θ ranges 15 to 70°C range in continuous scan mode. The scan rate was 0.04/sec with 35 KV and 25 Ma generator voltage and current.

2.4.4. Microscopy field emission scanning electron microscopy

FESEM was used to characterize mean particle size, the morphology of the AgNPs, FESEM produces clear images with spatial resolution down to 11/2 nm that are electrostatically less distorted, i.e., 3 and 6 times better than conventional SEM. Smaller-area contamination spots are often examined at electron accelerating voltages compatible with energy-dispersive X-ray spectroscopy. High-quality images are attained with minimal electrical charging of samples (voltages range is 0.5 to 30 kV). The powder sample and freeze-dried sample of the SNPs solution were sonicated with distilled water; a small drop of this sample was placed on a glass slide was allowed to dry. A thin layer of

platinum was coated to form the sample conductive Jeol. JSM-6480 L V FESEM machine was operated at a vacuum for the order of 10⁻⁵ torr. The accelerating voltage of the microscope was kept within the range of 10-20 kV.

2.4.5. Energy dispersive X-ray (EDX) analysis observation of SNPs

EDX was performed on the particles using JEOL-2100 high transmission electron microscope to confirm Ag presence and identify other elementary compositions of the particles. A minimal amount of the sample was drop-coated film and analyzed for the composition of the synthesized nanoparticles.

2.4.6. Particle size (diffuse light scattering method- DLS) with Zeta potential analysis

A laser diffraction method with a multiple scattering technique was used to know the particle size distribution of the sample. It was based on Mie-Scattering theory. A horn-type ultrasonic processor (Vibronics, VPLPI) was used to disperse Ag powder in water to determine particle size distribution. The data on particle size distribution was extracted in Zeta sizer version 6.20 Mall 052893, Malven Instrument.

2.5. Applications

2.5.1. Seed germination assay

An experiment was made to evaluate the effect of seaweed extract, *C. antennina* SNPs on the germinability of the candidate seeds *Vigna unguiculata* (L.) Walp, *Vigna radiata* (L.), and *Cicer arietinum* (L.) in a completely randomized design with duplicates (as per ISTA rules, 2014). The treatments in the experiment were taken in 25 %, 50 %, 75 %, and 100 % concentration of SNPs. This setup was kept at room temperature of 28 °C for 24 h. The seeds were soaked for 15 min in 5 % sodium hypochlorite for surface sterilization and then dipped in silver nanoparticles solution throughout the night. The control seeds were soaked in normal tap water and kept overnight. Then, the seeds were placed on the filter paper soaked with 5 mL SNP solution placed in the petriplates. The inoculated petriplates were incubated at room temperature. After 12 h, germination halted, and the germination percentage, mean germination time, germination index, relative root elongation, relative seed germination, and germination rate were estimated. Germination parameters were calculated using the following equations [31-33]. Germination percentage (GP %) = $(Gf/n) \times 100$ (1).

Where N_i is the number of germinated seeds until the i th day, D_i is the number of days from the start of the experiment until the i th counting, and n is the total number of germinated seeds.

$$\text{Germination Rate (GR)} = \sum N_i / \sum T_i N_i \quad (3)$$

where N_i is the number of newly germinated seeds at time T_i . $GR = (a/1) + (b-a/2) + (c-b/3) + \dots + (n-n-1/N)$ (4)

Relative root elongation (E) = (Mean root length with NPs) / (Mean root length with control) × 100

Germination index (GI) = (Relative seed germination) × (Relative root elongation) / 100

Where, Relative seed germination = (Seeds germinated with NPs) / (Seeds germinated with control) × 100.

Embryonic Axis Length (EAL) Study

The embryonic axis length, fresh and dry weight of the embryonic axis, and percentage increase/decrease over the control germinated seeds of *Vigna unguiculata* (L.) Walp, *Vigna radiata* (L.), and *Cicer arietinum* (L.) were calculated in 25 %, 50 %, 75 %, and 100 % concentrated SNPs solution of seaweed extract *C. antennina*.

2.5.2. Toxicity study of earthworm

The seaweed extract *C. antennina* was allowed to interact with earthworm *Lampito mauritii* at 25 %, 50 %, 75 %, and 100 % concentrations of SNPs solution and incubated at a room temperature of 28 °C. The time taken for the earthworm's mortality was noted and tabulated. Methanol, ethanol, rectified spirit, and silver nitrate solution served as the controls.

2.5.3. Antioxidant activity

2.5.3.1. 1, 1 Diphenyl 1-2-picrylhydrazyl free radical scavenging activity

The DPPH radical scavenging activity of different concentrations (100, 200, 300, 400, and 500 µg/mL) of algal extract and green synthesized SNPs of the seaweed extract *C. antennina* sample was measured [34]. The test samples (100-500 MI) were mixed with 0.8 MI of Tris-HCl buffer (pH 7.4), to which 1 MI DPPH (500 mM in ethanol) was added. The solution mixture was shaken vigorously well and kept for half an hour. A UV-Visible spectrophotometer (UV-160A; Shimadzu Company) was used to measure the absorbance of the resulting solution. Radical scavenging potential was expressed as IC₅₀ value, representing the concentration scavenged 50 % of the DPPH radicals. Scavenging activity of DPPH radical was calculated using the equation, percentage inhibition = $(A_{\text{control}} - A_{\text{sample}}) \times 100 / A_{\text{control}}$ where A_{control} is the absorbance of DPPH solution with the sample; A_{control} is a blank absorbance. Synthetic antioxidant ascorbic acid was used as a positive control.

3. Results and Discussion

Seaweeds are one of the most natural, sustainable resources within the marine ecosystem, contributing to food, feed, medicine, and sustainable development. It was estimated that about 90 % of the species of marine plants are algae, and about 50 % of the global photosynthesis is contributed from algae. The untapped biochemical compounds were present in these seaweeds, which could be a possible source of drug leads within the

future. India is a tropical South Asian country with around 7500 km of coastline area with divergent habitats and rich biota. The Southwest coast of India is a unique marine habitat crowded with varied seaweeds. Both intertidal and deepwater regions of the Indian coastal areas having approximately 841 species of marine algae. As a consequence of the increasing demand for biodiversity within the screening programs seeking curative drugs from natural products, there is now a greater interest in marine organisms, particularly algae. It is documented that many drugs are often prepared from marine sources, which could profitably be utilized in pharmaceutical industries. There is a growing demand and need for new bioactive drugs to control many malignant tumors.

The extract of *C. antennina* was green in color, but after adding AgNO_3 solution and incubated at room temperature, the color of the solution slowly changed into brown color. The change in color and intensity confirmed the reduction of Ag into AgNPs. A change in color could accompany a reduction in silver ions to silver nanoparticles. The synthesis of SNP was confirmed by visual observations. The color of the SNP varies from light yellow to golden brown based on the particle concentration in the mixture [35]. The color change in the reaction mixture was due to the excitation of surface plasmon vibration in the metal nanoparticles [16]. Many authors also reported time-dependent SNP production using algae as bioreagents. In Brown algae *Sargassum muticum* and *S. tenerrimum*, the SNP synthesis occurred within 20 min of reaction [36,37]. At the same time, *S. wightii* was taken only 10 min for synthesizing of SNP [38]. All the previous report concluded that the different exposure time is due to the different reducing agents. In the present study also the seaweed *C. antennina* changed to brown color. Due to the release of excess intracellular SNP or reduction of Ag ions by polysaccharides or enzymes secreted by algal thallus [39].

3.1. UV-vis spectroscopy analysis of *Chaetomorpha antennina*

UV vis absorption spectrum of *C. antennina* SNPs is shown in Fig. 2. The obtained spectrum was broad bell-shaped. The presence of many secondary metabolites in the solution leads to plasmon resonance of silver appeared at 452 nm. The SNPs synthesized was analyzed using UV-Vis spectroscopy to determine the characteristic of the peaks spectrum of SNPs wavelength. Based on the shape and size of nanoparticles, the characteristic of SNPs appears at a wavelength range of 400- 600 nm [40,41]. The absorption peaks around 410-430 nm for the surface plasma resonance (SPR) indicated nearly spherical-shaped SNP production. As per many kinds of literature, the SPR band of SNP can appear at any position in between the range of 410-490 nm wavelength. Generally, the position of the SPR band in UV-Vis spectra is based on the particle shape, size, interaction with the medium, local refractive index, and the charge transfer between particles and the medium. The SNPs absorption spectrum presents a maximum peaks height around 420- 450 nm with a blue or red shift with an increase in particle size was also reported [42]. In the present investigation, UV-Vis spectra of SNPs synthesized using the *C. antennina* algal extract evidenced the blue shift of the observation band around 452

nm. This information confirmed that these SNPs have formed in the extracts, where the Ag^+ has been reduced to Ag^0 . The presence of secondary metabolites and protein in the extracts played a vital role in both the reducing and capping mechanism of SNP formation [43]. The synthesized SNPs were highly stable, which was also confirmed by the zeta potential study. The spherical-shaped SNPs synthesized from *Ulva reticulata* and *Enteromorpha compressa* [44], *Turbinaria conoides* [45] exhibited intense peaks at 420 nm.

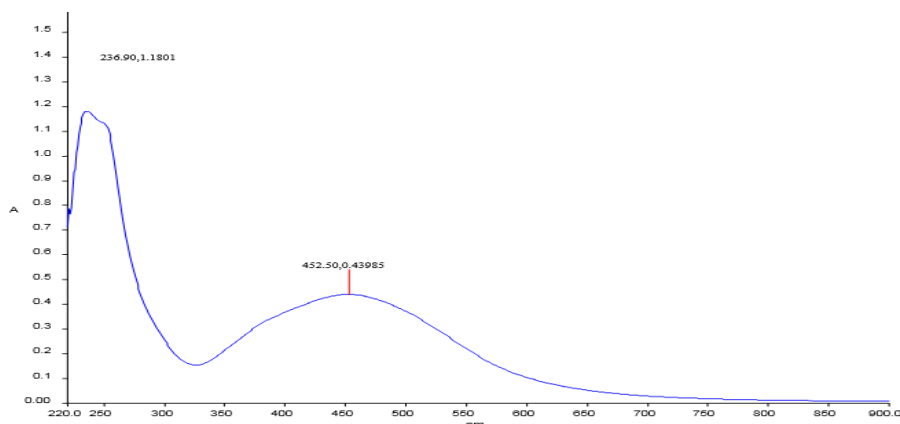


Fig. 2. UV-vis spectroscopy analysis of *Chaetomorpha antennina* SNPs.

The results obtained through FTIR analysis of the SNP peak values spectrum profile were illustrated in Fig. 3. The spectrum displayed 11 intense peaks at 3923, 3876, 3781, 3344, 2708, 2675, 2354, 2081, 1644, 1256 and 673 cm^{-1} in the region of 4000 cm^{-1} to 500 cm^{-1} . The absorption band at 3923, 3876, 3781, 3344, and 2708 cm^{-1} correspond to alcohol with O-H stretching. The peaks at 2675, 2354, and 2081 cm^{-1} evidenced the presence of carboxylic acid, carbon dioxide, and allen compounds with O-H, O=C=O, and C=C=C stretching, respectively. The sharp peak at 1644 cm^{-1} is mainly due to the N-H band stretching vibrations of amines. The absorption bands at 1256 and 673 cm^{-1} correspond to C-O stretching with functional aromatic ester and C-C bending of the alkene, respectively. Jabamalar and Judia [30] studied the crude extract of *Chaetomorpha* and analyzed it through FTIR. The absorption band at 3437 cm^{-1} corresponds to OH stretching vibration of polysaccharides, and the intense peak at 1636 cm^{-1} was equivalent to that of galactans. Similar results were obtained in the present FTIR study with *Chaetomorpha* SNPs [30].

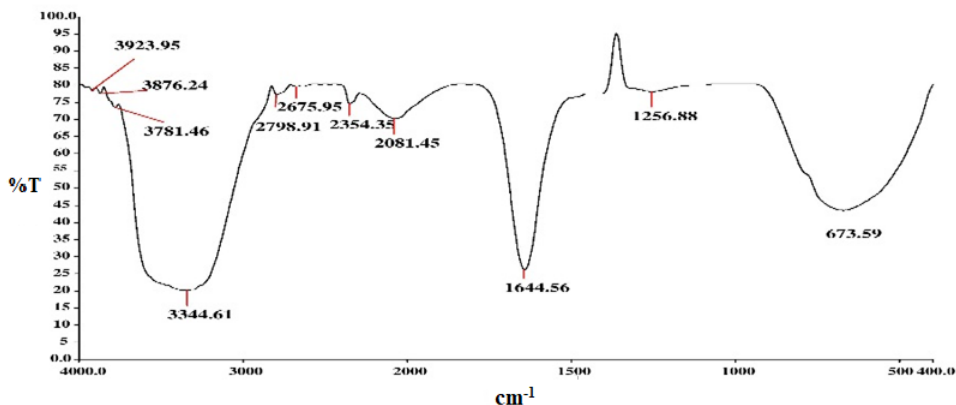


Fig. 3. FTIR analysis of *C. antennina* SNPs.

3.3. XRD analysis of chaetomorpha antennina SNPs

The structural characterization of SNPs synthesized from *C. antennina* has been performed by using XRD analysis. The typical XRD diffractogram obtained is shown in Fig. 4. According to the data and diffractogram, there is six distinct reflections at $32.20^\circ(18)$, $38.1^\circ(34)$, $45^\circ(19)$, $46.26^\circ(14)$, $64.39^\circ(18)$, and $72.4^\circ(10)$. In addition to this, ten unidentified peaks also appear in the XRD pattern. The typical XRD pattern showed that the extract contained a mixture of cubic and hexagonal structures of SNPs. The average SNPs size was 21 nm according to the peak's FWHM (full width at half minimum). The XRD spectra indicate that the formation of SNPs is crystalline, and the accumulation was formed due to the little action of stabilizing agent present in the algal extracts [46]. According to the present observation, the formatted Ag had nanoscale components and the calculated lattice constant, which is consistent with JCPDAS results [47].

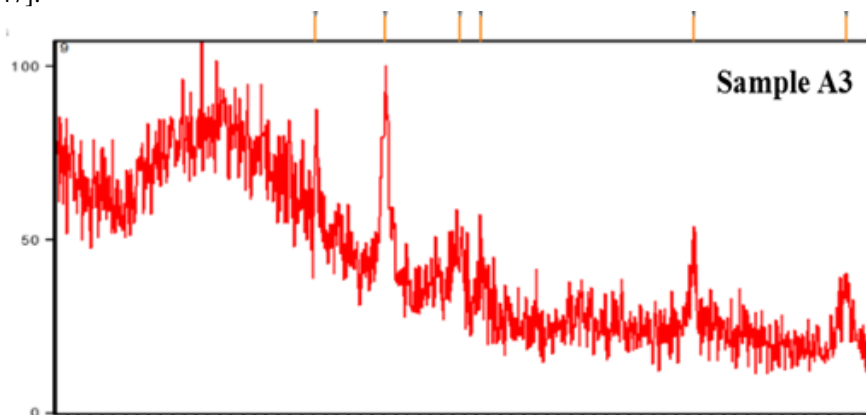


Fig. 4. XRD analysis of *C. antennina* SNPs.

3.4. FESEM study of *chaetomorpha antennina* SNPs

The size and shape of the green synthesized SNPs of *C. antennina* were studied by FESEM. Fig. 5 indicates that the synthesized SNPs were spherical in morphology with a size range from 69.99 to 99.15 nm. Among these, some SNPs were agglomerated. The difference in size may be due to the availabilities of various quantities and the nature of capping agents present in the sample. The FESEM image of *C. antennina* SNPs represented the morphological characterization of biosynthesized nanoparticles. It expressed the presence of high density, spherical and well-distributed SNPs synthesized from the extract. At the same time, previous studies of *C. antennina* showed the presence of high density, hexagonal, cubical SNPs with 256.2 nm diameter [48].

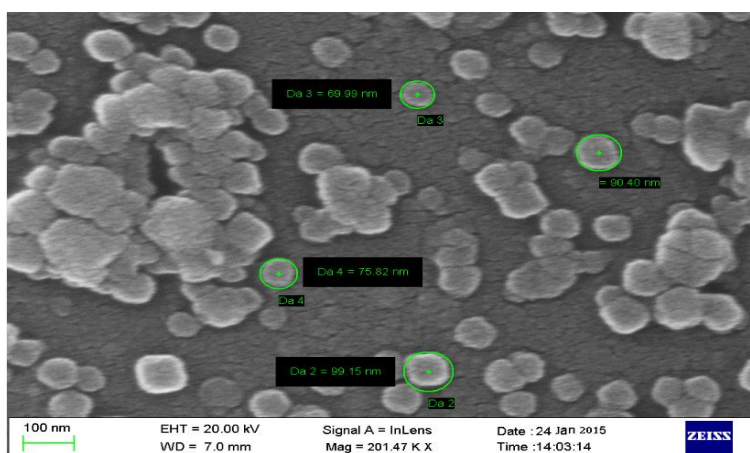


Fig. 5. FESEM image of *C. antennina* SNPs.

3.5. EDX analysis of *chaetomorpha antennina* SNPs

EDX analysis of SNPs obtained from *C. antennina* was performed for the confirmation of silver nanoparticles. The EDX analysis confirmed the presence of silver in the SNPs. A strong signal at 3 keV confirmed the presence of SNPs formation in the solution. The presence of a strong signal for silver atoms in all samples specified the purity of particles. The weak signals were observed for oxygen, sodium, magnesium, calcium, potassium, silicon, carbon, and aluminum are due to the presence of various biochemical molecules in the sample responsible for the SNPs synthesis (Fig. 6). The EDX analysis of *Chlamydomonas reinhardtii* [49], *Chaetomorpha* sp. [50] confirmed the presence of silver. A previous report found that carbon, oxygen, sulfur, potassium, sodium, and chlorine are elements in a minor amount in *Chaetomorpha* [51]. The present study of *Chaetomorpha* SNPs EDX analysis showed the presence of carbon, sodium, chlorine, calcium, oxygen, magnesium, silver potassium.

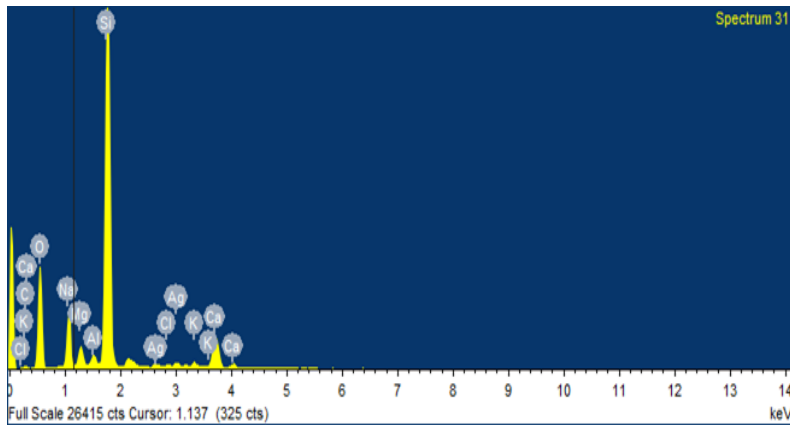


Fig. 6. EDAX report of *C. antennina* SNPs.

3.6. Particle size analysis of *Chaetomorpha antennina* SNPs

The DLS analysis of the *C. antennina* SNPs was presented in Fig. 7. The triplicate value of synthesized SNPs are 78.87, 78.08, and 78.81 nm, and the average size is 78.58 nm. The obtained zeta potential value of SNPs through the DLS method was -27.4 mV (Fig. 7 and Table 1). It is within the normal range (-20 to -30 mV), which indicates the stability of SNPs due to the electrostatic repulsion. Zeta potential is an essential factor in knowing the surface change of nanoparticles and projecting the stability of the synthesized SNPs. The zeta potential values of nanoparticles greater than $+25$ mV or greater than -25 mV typically have high degrees of stability. Generally, the normal range of zeta potential stability is -20 to 30 mV. Similar results were obtained from *C. antennina* Ag nanoparticles with a -31.4 mV zeta potential value [49]. This indicates the high stability of SNPs; it may be due to the more repulsive and attractive force that arises between nanoparticles [52]. A similar observation has also been reported for green synthesized SNPs of *Gracillaria cortica* with a zeta potential value of -26.2 mV [53].

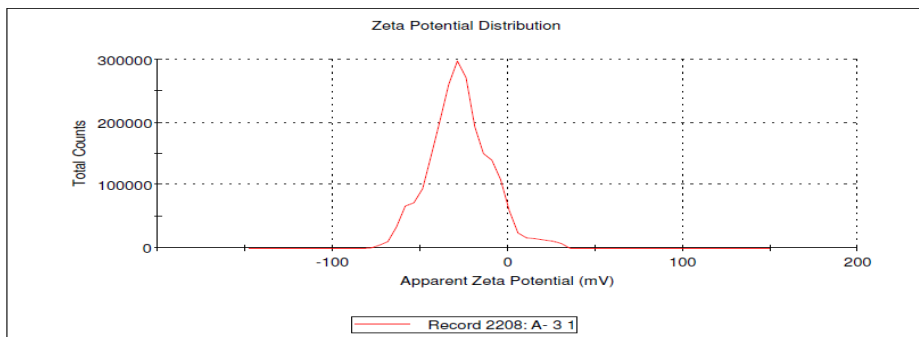


Fig. 7. Zeta potential of *C. antennina* SNPs.

Table 1. Summary of Zeta potential analysis of *C. antennina* SNPs.

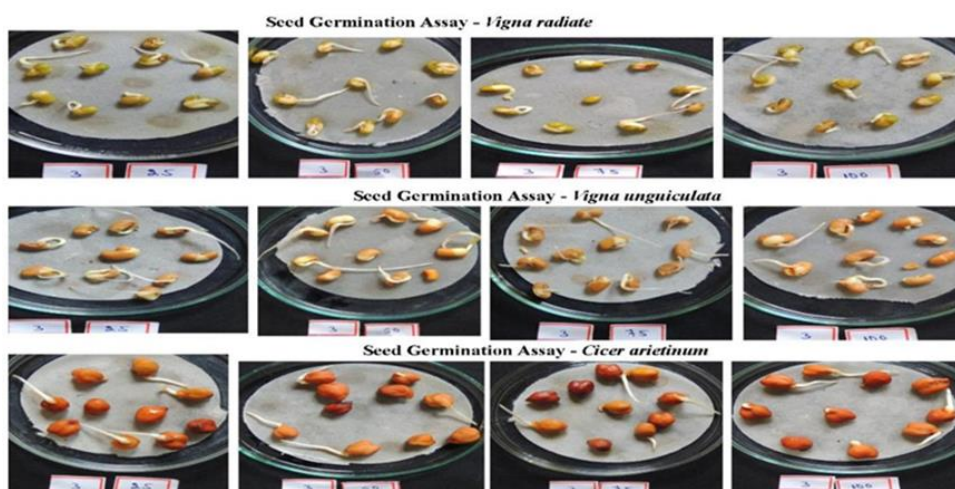
Record No.	Count rate (kcps)	Z-Potential (mV)	Mean (mV)	Area (%)	St.Dev (mV)	Z- Deviation (mV)	Conductivity (mS/cm)
1	270.9	-27.4	-27.4	100.0	17.5	17.5	0.349

3.7. Effect of *Chaetomorpha antennina* SNPs on seed germination potential

The SNPs obtained from *C. antennina* at different concentrations (25, 50, 75, 100 %) were used to study the seed germination potentials of *Vigna unguiculata* (L). Walp, *Vigna radiata* (L). R. Wilczek and *Cicer arietinum* L. A significant enhancement in germination percentage was noticed in all SNP concentrations against control for *V. unguiculata*. Here the percentage increase over control was +50.0, +33.33, +66.66 and +33.33 against 25, 50, 75 and 100 % SNPs concentration respectively. For *V. radiata* the highest germination percentage (100 %) was observed at 50 % SNP concentration against control (80 %). The increase in percentage over control was +25. The other SNPs concentrations (25%, 100%), also increased the seed germination percentage over control (+12.5, +12.5). However, there is no increase in seed germination percentage at 75 % SNP concentration compared to control (Table 2 and Fig. 8). The highest germination rate for *Cicer arietinum* seeds was 80 % observed with exposure to 100 % SNP concentration with an increase over control +60 %. The second best germination rate was observed at 75 % SNP concentration with 70 % germination and +40 % increases over control (Table 2 and Fig. 8). The control germination rate was 50 %. In previous studies, it had been reported that *Sargassum cinctum* seaweed-mediated SNPs had a positive and friendly effect and enhanced the growth of seedlings as well as seed germination percentage of *Abelmoschus esculentus* [48]. In the present study also *C. antennina* SNPs exhibited a positive effect on *V. unguiculata*, *V. radiata*, and *Cicer arietinum* seed germination. In comparison to water, biosynthesized SNPs showed a better effect on seed germination, which may be due to the availability of biochemical components, minerals, and antioxidants in the algal extract used to synthesize SNPs [48]. The SNPs synthesized from *Amphiroa anceps* also increased the seed germination percentage 75 % and 80 % in *Abelmoschus esculentus* and *Raphanus sativus* seeds, respectively [54]. The enhanced seed germination might be due to the efficient water, and nutrient uptake by the SNPs treated seeds, as the SNPs can penetrate the seed coat and may activate the embryo. The penetration of SNPs causes many new pores that remain helpful in absorbing nutrients efficiently and leads to fast germination [55,56]. This agrees with the study of Kingslin and Ravikumar [57] in *Padina tetrastromatica* SNPs role on seed germination.

Table 2. Seed germination assay of *C. antennina* SNPs.

Algae name	Plant name	Concentration	Germination (%)	Increase/Decrease over control
<i>C. antennina</i> SNPs	<i>Vigna unguiculata</i>	control	60	
		25 %	90	+50
		50 %	80	+33.33
		75 %	100	+66.66
		100 %	80	+33.33
	<i>Vigna radiata</i>	control	80	
		25 %	90	+12.5
		50 %	100	+25
		75 %	80	0
		100 %	90	+12.5
	<i>Cicer arietinum</i>	control	50	
		25 %	60	+20
		50 %	50	0
		75 %	70	+40
100 %		80	+60	

Fig. 8. Seed germination assay of *C. antennina* SNPs.

3.8. Embryonic axis study

The results obtained from the different concentrations (25, 50, 75 and 100 %) of *C. antennina* SNPs affect *Vigna unguiculata*, *V. radiata*, and *Cicer arietinum* EAL studies were displayed in Table 3. The parameters like embryonic axis length (EAL), mean percentage, increase or decrease of EAL over control, fresh weight (FWt) mean, dry weight (DWt) mean, water content means. Percentage increase or decrease of DWt over the control was tested and tabulated. The obtained results of *Vigna unguiculata* shows that the EAL increased up to +12.57 % in the 50 % SNP concentration compared to control. In

contrast, all other concentrations (25, 75 and 100 %) exhibited a decrease in the percentage of EAL (-1.142, -13.14, and -26.85 %) over the control. The sample's DWt expresses that the 50 % and 100 % SNP concentration only increases and 25 % and 75 % decrease in DWt over the control. In *Vigna radiata*, EAL results explained that all the concentrations did not increase the EAL over the control. The DWt results indicate that only 25% concentration increases (+31, +42 %), and all other concentrations did not show any positive results over the control. For *Cicer arietinum*, the results showed all the SNPs concentration enhanced EAL as well as DWt. The data of EAL increase was +49.47, 37.89, 38.94, and 37.89 and DWt +12.30, +19.84, +24.20 and +22.61 over the control against 25, 50, 75 and 100 % SNP concentration respectively (Table 3). EAL study of *Vigna unguiculata* and *V. radiata* exhibited a decrease in the EAL percentage over the control against *C. antennina* SNPs up to -26.85 and -29.72 % respectively. It clearly shows that SNPs have a toxic effect on embryonic axis development. This is in agreement with the earlier study of SNPs on maize plants [58]. Whereas, in *Cicer arietinum*, embryonic axis length increased against *C. antennina* SNPs up to +24.20 %. Regarding DWt and FWt of the embryonic axis, a significant increase in the DWt over the control was noted in *Vigna unguiculata*, *Cicer arietinum*, and 25 % SNP concentration. A decrease in the higher concentration of SNPs against DWt and FWt of embryonic axis in *V. radiata* may be due to the toxic effect of SNPs on embryonic axis length. Previous studies on the biological effects of AgNPs revealed higher toxicity [59]. High concentrations of silver ions can cause phytotoxic effects in several plants [60-62]. It is known that the physicochemical properties of particles viz shape, size, surface coating, and experimental conditions like concentration, time, method of exposure, and plant spaces are the major factors that influence AgNPs toxicity and uptake in plants [60,63,64]. The effect of *C. antennina* SNPs on embryonic axis growth appeared to be not related to the seed germination effect. Generally, the increase in seed germination percentage EAL also increased.

But in some cases, the seed germination percentage is not related to EAL and DWt. Similar results were obtained from the root length of corn, watermelon, and *Zucchini* plants, inhibiting corn root length and positive results for watermelon and *Zucchini* plants by SNPs [65]. Increased EAL with increased DWt over control agreed with a study in *Vicia faba* [66] and *Eruca sativa* [67] root length. Similar results were obtained on the *Pennisetum glaucum* plant, with higher seed germination in response to AgNPs, while seedling root elongation was inhibited [68]. The increase in dry weight and fresh weight of EAL in the present study was similar to that of corn, watermelon, and *Zucchini* plants seedling fresh weight and dry weight [65].

Table 3. Embryonic axis study of *C. antennina* SNPs

Algal sample	Plant name	Conc. of SNPs/ mean	EAL cm mean	% Increase/ decrease of EAL over C	FWt g mean	DWt g mean	Water g mean	% Increase/ decrease of DWt over C
<i>C. antennina</i> SNPs	<i>Vigna unguiculata</i>	control	3.5		0.150	0.062	0.088	
		25 %	3.46	-1.142	0.169	0.063	0.106	-1.612
		50 %	3.94	+12.57	0.197	0.068	0.129	+9.67
		75 %	3.04	-13.14	0.152	0.062	0.09	0
		100 %	2.56	-26.85	0.172	0.067	0.105	+8.06
	<i>Vigna radiata</i>	control	2.96		0.175	0.035	0.14	
		25 %	2.04	-31.08	0.140	0.046	0.094	+31.42
		50 %	2.06	-30.40	0.133	0.034	0.099	-2.85
		75 %	2.24	-24.32	0.152	0.032	0.12	-8.57
		100 %	2.08	-29.72	0.118	0.032	0.086	-8.57
<i>Cicer arietinum</i>	control	1.9		0.585	0.252	0.333		
	25 %	2.84	+49.47	0.664	0.283	0.381	+12.30	
	50 %	2.62	+37.89	0.627	0.302	0.325	+19.84	
	75 %	2.64	+38.94	0.706	0.313	0.393	+24.20	
	100 %	2.62	+37.89	0.656	0.309	0.347	+22.61	

3.9. Antioxidant activity

The antioxidant activity of aqueous extracts of *C. antennina* algal SNPs and algal extracts was evaluated using DPPH scavenging activity. The result of the DPPH assay and graphical representation of SNPs and algal extract samples were presented (Table 4). In both algal extract and SNPs samples, the DPPH values were increased in a dose-dependent manner. The DPPH values of *C. antennina* algal SNPs and algal extract was 40.6, 45.0, 49.2, 51.5, 52.0 and 45.5, 45.7, 46.8, 47.2, 50 % against the concentrations 100, 200, 300, 400 and 500 µg/mL respectively. The lowest IC₅₀ value was observed in algal SNP extract 584.13 µg/mL, compared to algal extract alone (611.0 µg/mL) (Table 4). The antioxidant activity of the nanoparticles is mainly due to the presence of organic biomolecules, which act as a chelating agent during the synthesis of nanoparticles [69].

Moreover, studies revealed that the reasons for the free radical scavenging activity of biosynthesized nanoparticles are the high surface-to-volume ratio [70,71]. It is believed that the synthesized nanoparticle from natural compounds have much antioxidant activity, and it is linked with the reduction of toxicity of the cells more efficiently. Further, these flavonoids exist as glycosides, contain many phenolic hydroxyl groups [72]. Generally, the *Chaetomorpha* sp. are have more amount of polyphenolic compounds [73,74]. The presence of phlorotannins, bipolar hydrophilic polyphenolic compounds, which function as a major antioxidant, helps the algae repel oxidative stress [75]. The antioxidant potential of *Chaetomorpha* is mainly due to the presence of phenols and flavonoids [76]. The DPPH assay revealed the antioxidant activity IC₅₀ value 611.0 µg/mL in aqueous crude extracts and 384.13 µg/mL for SNPs. These results were supported by the previous studies that found higher antioxidant properties in external extracts [75-77]. Jebamalar and Judia Harriet Sumathy [30] also confirmed the antioxidant activities of *C. antennina* methanol extract and its polysaccharides.

Table 4. DPPH radicalscavenging activity of *C. antennina* SNPs.

Algae Name	Components	Concentration ($\mu\text{g/mL}$) / OD value					IC50
		100	200	300	400	500	
<i>C. antennina</i> SNPs	AgNPs	1.274	1.180	1.090	1.039	1.029	384.13
	%	40.6	45.0	49.2	51.6	52.0	
	Extract	1.170	1.165	1.141	1.132	1.074	611.0
	%	45.5	45.7	46.8	47.2	50.0	
Control		2.148					

3.10. Toxicology study of ten macro algal SNPs on *Lampito mauritii* (earthworm)

The Petridish filter papers study of *C. antennina* algal SNPs acute toxicity to earthworms was conducted using four different concentrations of SNPs (25, 50, 75, and 100 %). There was no death in the Petridish filter papers study of *L. mauritii* earthworms in control maximum up to 120 min. However, the deaths occurred within 3 min of exposure to *C. antennina* SNPs in the lower concentrations 25 % (Fig. 9). In this increase in concentrations of SNPs decrease the death time of earthworms was observed. The death time of solvent control methanol, sprit, ethanol, and AgNO_3 were 1.39, 2.05, 2.25, and 3 min, respectively.

The earthworm death time was noticed in the 25, 50, 75, and 100 % SNPs concentration. Among these concentrations, earthworm death occurred within 3 min of exposure at 25 % concentration, whereas in control, no death has occurred up to 120 min. Furthermore, the dose-dependent death time was noticed, i.e., an increase in the concentration decrease in the death time of earthworms. Previous report results also explained the adverse effects of AgNP on the growth and proliferation of earthworms [78]. But SNPs obtained from *Mentha arvensis* showed that lower concentrations did not affect the growth and proliferation of earthworms [79]. Significant toxic effects of earthworm in Petridish filter paper test and deaths occurred at all the tested heavy metal concentrations [80]. In the present study, the death of earthworm occurred within 3 min of incubation at a lower concentration. This might be due to the higher SNP concentration (25, 50, 75, and 100 %). At the same time, the solvent control death time was 1.39, 2.05, 2.25, and 3 min against methanol, sprit, ethanol, and AgNO_3 , respectively. So, the present result is equal to the AgNO_3 death time of earthworms.

Fig. 9. Toxicology study of *C. antennina* SNPs.

5. Conclusion

This study demonstrated the noteworthy recombination of AgNPs utilizing macroalgae *Chaetomorpha antennina* aqueous extract. This AgNP production relied heavily on the bioactive compounds found in the algae. Silver nanoparticles were confirmed by UV, FTIR, XRD, FESEM, EDX, Zeta potential. The silver nanoparticles created this way do not contain toxic reagents, making them a potential candidate for biomedical applications. The synthesized silver nanoparticles by using *C. antennina* bioreagent is an eco-friendly and cost-effective procedure with antioxidant activity.

References

1. S. Roy and TK. Das, Int. J. Plant Biol. Res. **3**, 1044 (2015).
2. S. Ahmad, S. Munir, N. Zeb, A. Ullah, B. Khan, J. Ali, M. Bilal, M. Omer, M. Alamzeb, S. M. Salman, and S. Ali, Int. J. Nanomedicine **14**, 5087 (2019). <https://doi.org/10.2147/IJN.S200254>
3. S. Basu and H. S. Samanta, J. Ganguly, Soft Mater **16**, 7 (2018). <https://doi.org/10.1080/1539445X.2017.1368559>
4. S. Carabineiro, Molecules, **22**(5), 857 (2017). <https://doi.org/10.3390/molecules22050857>
5. H. Fukui, M. Naito, T. Yokoyama, K. Hosokawa, and K. Nogi, Editors. Nanoparticle Technology Handbook, 3rd Edition (Elsevier, Japan), pp. 845-877.
6. D. Bharathi, M. D. Josebin, S. Vasantharaj, and V. Bhuvaneshwari, J. Nanostruct. Chem. **8**, 83 (2018). <https://doi.org/10.1007/s40097-018-0256-7>
7. J. B. Fathima, A. Pugazhendhi, M. Oves, and R. Venis, J. Mol. Liq. **260**, 1 (2018). <https://doi.org/10.1016/j.molliq.2018.03.033>
8. P. Sharma, D. Bhatt, M. Zaidi, P. P. Saradhi, P. Khanna, and S. Arora, Appl. Biochem. Biotechnol. **167**, 2225 (2012). <https://doi.org/10.1007/s12010-012-9759-8>
9. J. Zhang, G. Si, J. Zou, R. Fan, A. Guo, and X. J. Wei, Food Sci. **82**, 1861 (2017). <https://doi.org/10.1111/1750-3841.13811>
10. M. Sivaramakrishnan et.al., SN Appl. Sci. **1**, 208 (2019). <https://doi.org/10.1007/s42452-019-0221-1>
11. S. S. Shankar, A. Ahmad, and M. Sastry, Biotechnol. Prog. **19**, 1627 (2003). <https://doi.org/10.1021/bp034070w>
12. B. Amkamwar, C. Damle, A. Ahmad, and M. Sastry J. Nanosci. Nanotechnol. **5**, 1666 (2005). <https://doi.org/10.1166/jnn.2005.184>
13. P. S. Chandran, M. Chaudhary, R. Pasricha, A. Ahmad, and M. Sastry, Biotechnol. Prog. **22**, 577 (2006). <https://doi.org/10.1021/bp0501423>
14. S. Li, Y. Shen, A. Xie, X. Yu, L. Qui, L. Zhang, and Q. Zhang, Green Chem. **9**, 852 (2007). <https://doi.org/10.1007/s13204-012-0125-5>
15. V. Ranjitha, K. Kalimuthu, V. Chinnadurai, Y. S. Juliet, and M. Saraswathy, Pharmacognosy Magazine **14**, S147 (2017). https://doi.org/10.4103/pm.pm_64_17
16. K. Govindaraju, V. Kiruthiga, V. G. Kumar, and G. Singaravelu, J. Nanosci. Nanotechnol. **9**, 5497 (2009). <https://doi.org/10.1166/jnn.2009.1199>
17. A. Nabikhan, K. Kandasamy, A. Raj, and A. N. Alikunhi, Colloids Surf. B. **79**, 488 (2010). <https://doi.org/10.1016/j.colsurfb.2010.05.018>
18. S. R. Kumar, C. Malarkodi, and S. Venkatkumar, Asian J. Pharm. Clin. Res. **10**, 190 (2017). <https://doi.org/10.22159/ajpcr.2017.v10i2.15127>
19. P. Bhuyar, M. H. A. Rahim, S. Sundararaju, R. R. Raj, G. P. Maniam, and N. Govindan, Beni-suef University J. Basic Appl. Sci. **9**, 1 (2020). <https://doi.org/10.1186/s43088-019-0031-y>
20. M. S. Tierney, A. K. Croft, and M. Hayes, Bot Mar. **53**, 387 (2010). <https://doi.org/10.1515/bot.2010.044>

21. A. M. S. Mayer, A. D. Rodriguez, R. G. S. Berlinck, and N. Fusetani, *Comp. Biochem. Physiol. C: Toxicol. Pharmacol.* **153**, 191 (2011). <https://doi.org/10.1016/j.cbpc.2010.08.008>
22. D. J. Faulkner, *Nat. Prod. Rep.* **17**, 1 (2000). <https://doi.org/10.1039/a909113k>
23. D. J. Faulkner, *Antonie Van Leeuwenhoek* **77**, 135 (2000). <https://doi.org/10.1023/A:1002405815493>
24. A. B. D. Rocha, R. M. Lopes, and G. Schwartzmann, *Curr. Opin. Pharmacol.* **1**, 364 (2001). [https://doi.org/10.1016/S1471-4892\(01\)00063-7](https://doi.org/10.1016/S1471-4892(01)00063-7)
25. G. Schwartzmann, A. B. D. Rocha, G. J. S Berlinck, and J. Jimenol, *Lancet Oncol.* **2**, 221 (2001). [https://doi.org/10.1016/S1470-2045\(00\)00292-8](https://doi.org/10.1016/S1470-2045(00)00292-8)
26. S. Choudhury, A. Sree, S. C. Mukherjee, P. Pattnaik, and M. Bapuji, *Asian Fisheries Sci.* **18**, 285 (2005). <https://doi.org/10.33997/j.afs.2005.18.3.009>
27. S. Ravikumar, G. Ramanathan, S. J. Inbaneson, and A. Ramu, *Parasitol. Res.* **108**, 107, (2011). <https://doi.org/10.1007/s00436-010-2041-5>
28. S. Palanisamy and S. Sellappa, *Jundishapur J. Microbiol.* **12**, 411 (2012).
29. D. Abhishek, P. Jyoti, D. Savan, and C. Sumitra. *J. Pharm. Phytochem.* **7**, 3863 (2018).
30. Jebamalar and J. H. Sumathy. *Int. J. Eng. Tech.* **4**, 405 (2018).
31. G. Singaravelu, J. Arokiyamari, V. G. kumar, and K. Govindaraju, *Colloids Surfaces B: Biointerfaces* **57**, 97 (2007). <https://doi.org/10.1016/j.colsurfb.2007.01.010>
32. M. S. Taga, E. E. Miller, and D. E.Pratt. *J. Am. Oil Chem. Soc.* **61**, 928 (1984). <https://doi.org/10.1007/BF02542169>
33. K. N. Thakkar, S. S. Mhatre, and R. Y. Parikh, *Nanomedicine* **6**, 257 (2010). <https://doi.org/10.1016/j.nano.2009.07.002>
34. A. P. Kulkarni, S. M. Aradhya, and S. Divakar, *Food Chem.* **87**, 551 (2004). <https://doi.org/10.1016/j.foodchem.2004.01.006>
35. S. Saha, D. Chattopadhyay, and K. Acharya, *Dig. J. Nanomater. Biostruct.* **6**, 1526 (2011).
36. S. Azizi, F. Namvar, M. Mahdavi, M. B. Ahmad, and R. Mohamad, *Materials* **6**, 5942 (2013). <https://doi.org/10.3390/ma6125942>
37. P. Kumar, S. S. Selvi, A. L. Prabha, K. Premkumar, R. S. Ganeshkumar, and M. Govindaraju, *Nano Biomed. Eng.* **4**, 12 (2012). <https://doi.org/10.5101/nbe.v4i1.p12-16>
38. S. Sunitha, A. Nageswara, Rao1, L. S. Abraham, E. Dhayalan, R. Thirugnanasambandam, and V. G. Kumar, *J. Chem. Pharm. Res.* **7**, 191 (2015).
39. P. Roychoudhury, P. K. Gopal, S. Paul, and R. Pal, *J. Appl. Phycol.* **28**, 3387 (2016). <https://doi.org/10.1007/s10811-016-0852-1>
40. R. Vasireddy, R. Paul, and A. K. Mitra, *Nanomater. Nanotechnol.* **2**, 8 (2012). <https://doi.org/10.5772/52329>
41. S. S. Shankar, A. Rai, A. A. Ahmad, and M. Sastry, *J. Coll. Interface Sci.* **275**, 496 (2004). <https://doi.org/10.1016/j.jcis.2004.03.003>
42. S. Pal, Y. K. Tak, and J. M. Song, *Appl. Environ. Microbiol.* **73**, 1712 (2007). <https://doi.org/10.1128/AEM.02218-06>
43. G. Marslin, K. Siram, Q. Maqbool, R. K. Selvakesavan, D. Kruszka, P. Kachlicki, G. Franklin, *Materials* **11**, 940 (2018). <https://doi.org/10.3390/ma11060940>
44. P. K. Dhanalakshmi, A. Riyazulla, R. Rekha, I. S. Poonkod, and N. Thangaraju, *Phykos* **42**, 39 (2012).
45. S. Rajeshkumar, C. Kannan, and G. Annadurai, *Drug Invention Today* **4**, 511 (2012).
46. S. A. David, K. M. Ponvel, M. A. Fathima, S. Anita, J. Ashli, and A. Athilakshmi, *J. Nat. Prod. Plant Resour.* **4**, 1 (2014).
47. P. Prakash, P. Gnanaprakasam, R. Emmanuel, S. Arokiyaraj, and M. Saravanan, *Colloids Surfaces B: Biointerfaces* **1**,108, 255 (2013). <https://doi.org/10.1016/j.colsurfb.2013.03.017>
48. S. Roy and P. Anantharaman, *J. Nanomed. Nanotechnol.* **8**, 467 (2017). <https://doi.org/10.4172/2157-7439.1000467>
49. I. Barwal, P. Ranjan, S. Kateriya, and S. C. Yadav, *J. Nanobiotechnol.* **9**, 56 (2011). <https://doi.org/10.1186/1477-3155-9-56>

50. S. H. Haq, G. Al-Ruwaished, M. A. Al-Mutlaq, S. A. Naji, M. Al-Mogren, S. Al-Rashed, Q. T. Ain, A. A. Al-Amro, A. Al-Mussallam, Scientific Reports **9**, 18906 (2019).
<https://doi.org/10.1038/s41598-019-55309-1>
51. A. Navarro, A. Hernandez-Vega, M. Masud, L. Robertson, and L. Diaz-Vazquez. Environments **4**, 1 (2016). <https://doi.org/10.3390/environments4010001>
52. J. Lee, H. Y. Kim, H. Zhou, S. Hwany, K. Koh, D. W. Ham, and J. Lee, J. Master Chem. **21**, 13316 (2011). <https://doi.org/10.1039/c1jm11592h>
53. P. Kumar, S. S. Selvi, and M. Govindaraju, Appl. Nanosci. **3**, 495 (2013).
<https://doi.org/10.1007/s13204-012-0151-3>
54. S. Roy and P. Anantharaman, J. Nanomed. Nanotechnil. **9**, 492 (2018).
<https://doi.org/10.4172/2157-7439.1000492>
55. C. Srinivasan and R. Saraswathi, Curr. Sci. **99**, 274 (2010).
56. L. Zheng, F. Hong, S. Lu, and C. Lin, Biotech.Trace Element Res. **104**, 82 (2005).
<https://doi.org/10.1385/BTER:104:1:083>
57. A. Kingslin and P. Ravikumar, World J. Pharm. Phram. Sci. **5**, 1304 (2016).
58. W. Mahakham, P. Theerakulpisut, S. Maensiri, S. Phumying, and A. K. Sarmah, Sci. Total Environ. **573**, 1089 (2016). <https://doi.org/10.1016/j.scitotenv.2016.08.120>
59. L. Yin, , Y. Cheng, B. Espinasse, B. P. Colman, M. Auffan, M. Wiesner, J. Rose, J. Liu, and E. S. Bernhardt, Environ. Sci. Technol. **45**, 2360 (2011). <https://doi.org/10.1021/es103995x>
60. P. Cvjetko, A. Milošić, A. –M. Domijan, I. V. Vrček, S. Tolić, P. P. Štefanić, I. Letofsky-Papst, M. Tkalec, and B. Balen, Ecotoxicol. Environ. Safety **137**, 18 (2017).
<https://doi.org/10.1016/j.ecoenv.2016.11.009>
61. L. R. Pokhrel and B. Dubey, Sci. Total Environ. **452**, 321 (2013).
<https://doi.org/10.1016/j.scitotenv.2013.02.059>
62. J. Yasur and P. U. Rani, Environ. Sci. Pollut. Res. **20**, 8636 (2013).
<https://doi.org/10.1007/s11356-013-1798-3>
63. K. Kettler, K. Veltman, D. Van de Meent, A. Van Wezel, and A. J. Hendriks, Environ. Toxicol.Chem. **33**, 481 (2014). <https://doi.org/10.1002/etc.2470>
64. R. Amooaghaiea, M. R. Saeri, and M. Azizi, Ecotox. Environ. Safety **120**, 400 (2015).
<https://doi.org/10.1016/j.ecoenv.2015.06.025>
65. M. Zainab, Almutairi, and A. Alharbi, J. Adv. Agricul. **4**, 280 (2015).
<https://doi.org/10.24297/jaa.v4i1.4295>
66. E. A. Abdul–Azeem and B. A. Elsayed, Ny. Sci. J. **6**, 148 (2013).
67. C. Vannini, G. Domingo, E. Onelli, B. Prinsi, M. Marsoni, L. Espen, and M. Bracal, PLoS One **8**, ID e6875 (2013). <https://doi.org/10.1371/journal.pone.0068752>
68. A. Parveen and S. Rao, J. Clust. Sci. **26** (2014). <https://doi.org/10.1007/s10876-014-0813-2>
69. H. Umar, D. Kavaz, and N. Rizaner, Int. J. Nanomed. **14**, 87 (2019).
<https://doi.org/10.2147/IJN.S186888>
70. G. Balasubramani, R. Ramkumar, N. Krishnaveni, A. Pazhanimuthu, T. Natarajan, R. Sowmya, and P. Perumal, J. Trace. Elem. Med. Bot. **30**, 83 (2015).
<https://doi.org/10.1016/j.jtemb.2014.11.001>
71. M. K. Swamy, M. S. Akhter, S. K. Mohanty, and U. R. Sinniah, Spectrochim Acta. A, Mol. Biomol. Spectrosc. **151**, 939 (2015). <https://doi.org/10.1016/j.saa.2015.07.009>
72. C. P. Anokvvuru, I. Esiaba, O. Ajibaye, and A. O. Adesuyi, Res. J. Med. Plants **5**, 557 (2011).
<https://doi.org/10.3923/rjmp.2011.557.566>
73. M. Farasat, R. K. Nejad, S. Nabavi, and F. Namjoyan, Braz. Archiv. Biol. Technol. **56**, 921 (2013). <https://doi.org/10.1590/S1516-89132013000600005>
74. Q. Wu, L. Liu, A. Miron B. Klimová, D. Wan, and K. Kuča, Arch. Toxicol. **90**, 1817 (2016).
<https://doi.org/10.1007/s00204-016-1744-5>
75. P. Senthilkumar and S. Sudha, J. Microbiol. **5**, 411 (2012). <https://doi.org/10.5812/jjm.3400>
76. S. Thanigaivel, S. Vijayakumar, A. Mukherjee, N. Chandrasekaran, and J. Thomas, Aquaculture **433**, 467 (2014). <https://doi.org/10.1016/j.aquaculture.2014.07.003>

77. S. H. Haq, G. Al-Ruwaished, M. A. Al-Mutlaq, S. A. Naji, M. Al-Mogren, S. Al-Rashed, Q. T. Ain, A. A. Al-Amro, A. Al-Mussallam, Scientific Reports **9**, 18906 (2019).
<https://doi.org/10.1038/s41598-019-55309-1>
78. L. H. Heckmann, M. B. Hougaard, D. S. Sutherland, H. Autrap, F. Besenbacher, and J. J. Scot-Fordsmand, Ecotoxicology **20**, 226 (2011). <https://doi.org/10.1007/s10646-010-0574-0>
79. P. Das, C. R. Chowdhori, and S. Barman, NASS J. Agricul. Sci. **1**, 18 (2019).
80. P. Muangphra and R. Gooneratne, Appl. Environ. Soil Sci. **2011**, 1 (2011).
<https://doi.org/10.1155/2011/218929>